

The Optimal Axial Interval in Estimating Depth from Defocus

Yoav Y. Schechner

Department of Electrical Engineering
Technion - Israel Institute of Technology
Haifa, Israel 32000
yoavs@tx.technion.ac.il

Nahum Kiryati

Dept. of Electrical Engineering - Systems
Faculty of Engineering, Tel-Aviv University
Ramat Aviv, Israel 69978
nk@eng.tau.ac.il

Abstract

We analyze the effect of perturbations on the estimation of Depth from Defocus (DFD) implemented by changing the focus setting (e.g., axially moving the sensor). The analysis yields the optimal change of focus setting, and the spatial frequencies for which estimation is most robust. For stable estimation at all spatial frequencies, the change in focus setting should be less than twice the depth of field. For the most robust estimation in the highest spatial frequencies the axial interval should be equal to the depth of field.

1. Introduction

In recent years, range imaging based on the limited depth of field (DOF) of lenses has been gaining popularity. Depth from Defocus (DFD) is an elegant method since it enables depth estimation based on only two images of the scene, taken from the same viewpoint. The defocus blur is made different in the two images by changing the internal settings of the imaging system. The effect of those changes on the defocus blur can be modeled either empirically or by analysis. This model provides the necessary a-priori knowledge for the estimation of the defocus blur and consequently the distance of the object from the imaging system. One way to change the defocus blur between images is to change the aperture size. Another approach is to change the focus setting of the system. For example, the sensor array can be moved axially between image acquisitions. The latter implementation is considered in this paper.

It has been shown [16] that DFD is a manifestation of the principle of geometric triangulation. However, the two-dimensionality of the lens aperture (in contrast to the one-dimensional stereo or motion baseline), makes depth estimation based on two images potentially more robust in DFD than in stereo [16]. Our general goal is to exploit this potential advantage. This requires the robustness of DFD to be studied in detail. Optimizing the change of internal settings

in the imaging system was investigated in [15]. In that work the optimal ratio between the effective blur-diameters in the images was derived. However, the result was dependent on the image contents. The issue of estimation stability was also considered in [21]. Stability at all spatial frequencies was required. This guided the choice of axial movement of the sensor between the image acquisitions, regardless of the image content. The numeric derivation of the axial interval in [21] was oriented towards a specific estimation algorithm (rational operators).

In this paper, we study the robustness of DFD in a general framework by analyzing the influence of perturbations in each spatial frequency of which the image is composed. We show that certain frequency components are most useful for range estimation, while others do not provide stable contributions. It is possible to accomplish stable depth estimation in frequency (or defocus) bands that contain some unstable frequency components, by filtering out the problematic components. This extends the results of [21].

Our analysis also reveals a new property of depth of field (DOF): it is the optimal interval between focus-settings in depth-from-defocus in terms of robustness. We also show that if the interval used is larger than the DOF by a factor of 2 or higher, the estimation process can be unstable. This sets limits on the interval between focus settings that ensures robust operation of DFD.

2. Error propagation

Consider the imaging system sketched in Fig. 1. The sensor at distance \tilde{v} behind the lens (of focal length F) can image in-focus a point at distance \tilde{u} in front of the lens. An object point at distance u is defocused, and its image is a blur-circle of radius r in the sensor plane. For simplicity we adopt the common assumption that the imaging system is invariant to transversal shift. This is approximately true for paraxial systems, where the angles between light rays and the optical axis are small. The diameter of the blur-circle

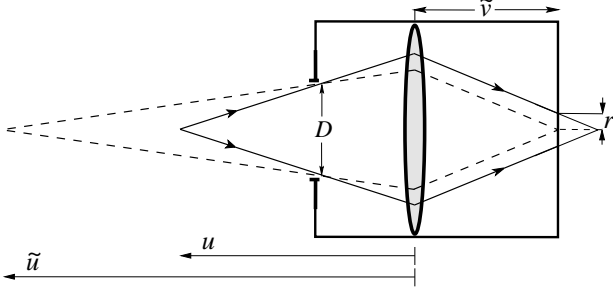


Figure 1. The imaging system is tuned to view in focus object points at distance \tilde{u} . The image of an object point at distance u is a blur circle of radius r in the sensor plane.

$d = 2r$ is a function of the distance u ,

$$d = f(u) . \quad (1)$$

For example, in a telecentric system [11, 21], as sketched in Fig. 1, with the aperture stop at distance F from the lens,

$$f(u) = \frac{D}{F} \left| \tilde{v} - \frac{Fu}{u-F} \right| , \quad (2)$$

where D is the diameter of the aperture stop [18]. For other systems the relation $f(u)$ may be different. In a simple-lens system $f(u) = D|uF - \tilde{v}u + F\tilde{v}|/(Fu)$. To maintain generality, we will not use a specific form of this function throughout this paper. In DFD, at least two images of the scene are acquired and compared. The comparison yields an estimate of the diameter d of the blur-circle in one of the images, which through the inversion of Eq. (1) leads to an estimate of the distance u .

We now analyze the response of DFD to perturbations by concentrating on the effect of a perturbation in some spatial frequency component of the image, as we suggested in [17]. The perturbation affects the estimated transfer function between the images, which in turn causes an error in the estimated blur-diameter. This leads to an error in the depth estimation. We note that studying the behavior of each spectral component has an algorithmic ground in DFD: there are several methods [2, 6, 13, 14, 21] which rely directly on the frequency components or on frequency bands [14], fitting a curve or a model to data obtained in several frequencies. Thus, even though the analysis refers to a single spatial frequency component, its results are relevant to general images.

Suppose that the pinhole image of the scene (in which everything is in focus) is g_0 . Let the two finite-aperture (thus defocus blurred) images be $g_1 = g_0 \star h_d$ and $g_2 = g_0 \star h_{d+\Delta d}$. Δd is the change in the blur-diameter due to

the known axial shift in sensor position. We assume that geometric changes in magnification are compensated or do not take place (e.g. by the use of a telecentric system [11, 21]). Moreover, in telecentric systems Δd is invariant to the focus settings and the object depth u [11, 18]. Therefore, the results presented here are best applicable to telecentric systems. In the frequency domain, let one image be

$$G_1(\nu) = G_0(\nu)H_d(\nu) + N_1(\nu) , \quad (3)$$

where ν denotes a spatial frequency component and $N_1(\nu)$ is a perturbation. The other image is

$$G_2(\nu) = G_0(\nu)H_{d+\Delta d}(\nu) . \quad (4)$$

If there is no perturbation, the two images satisfy

$$G_2(\nu)H_d(\nu) - G_1(\nu)H_{d+\Delta d}(\nu) = 0 . \quad (5)$$

We wish to estimate \hat{d} by searching for the value that satisfies

$$G_2(\nu)H_{\hat{d}}(\nu) - G_1(\nu)H_{\hat{d}+\Delta d}(\nu) = 0 . \quad (6)$$

Assume for a moment that $H_d(\nu) \neq 0$, and define

$$H(\nu) = \frac{H_{d+\Delta d}(\nu)}{H_d(\nu)} , \quad \hat{H}(\nu) = \frac{H_{\hat{d}+\Delta d}(\nu)}{H_{\hat{d}}(\nu)} . \quad (7)$$

Usually constraint (6) cannot be satisfied by the same \hat{d} at all frequencies, hence a common method [4] is to minimize a MSE criterion such as

$$\begin{aligned} E^2 &= \int_{\nu} |G_2(\nu) - \hat{H}(\nu)G_1(\nu)|^2 d\nu = \\ &= \int_{\nu} |G_0(\nu)H_d(\nu)|^2 \left| H(\nu) - \hat{H}(\nu) \left[1 + \frac{N_1}{G_0 H_d} \right] \right|^2 d\nu . \end{aligned} \quad (8)$$

This is achieved by looking for the extremum points

$$\begin{aligned} 0 &= -\frac{\partial(E^2)}{\partial \hat{d}} = 2Re \int_{\nu} |G_0(\nu)H_d(\nu)|^2 \left[1 + \frac{N_1^*(\nu)}{G_0^* H_d^*} \right] \cdot \\ &\cdot \left\{ H(\nu) - \hat{H}(\nu) \left[1 + \frac{N_1}{G_0 H_d} \right] \right\} \frac{\partial \hat{H}^*(\nu)}{\partial \hat{d}} d\nu . \end{aligned} \quad (9)$$

The locations of minima of E^2 depend on the spectral composition of the signal and noise. Consider a signal made of a single frequency ν

$$G_0(\nu') = G(\nu)\delta(\nu - \nu') . \quad (10)$$

If at that frequency $\partial \hat{H}^*(\nu)/\partial \hat{d} = 0$, the estimation of \hat{d} is ill posed. Otherwise, nulling the integrand yields

$$H_{\hat{d}+\Delta d}(\nu)H_d(\nu) = H_{\hat{d}}(\nu)H_{d+\Delta d}(\nu) - \frac{N_1(\nu)}{G_0(\nu)}H_{\hat{d}+\Delta d}(\nu) \quad (11)$$

Eq. (11) can be written as

$$\hat{H}(\nu) = H(\nu) \left[1 + \frac{N_1(\nu)}{G_0(\nu)H_d(\nu)} \right]^{-1}. \quad (12)$$

The true blur-diameter d controls the transfer function $H(\nu)$ between the images. Basically, the estimate \hat{d} is deduced from measurements of $H(\nu)$. However, due to the perturbation, a different $\hat{H}(\nu)$ is measured.

$$\begin{aligned} \frac{\partial \hat{H}(\nu)}{\partial |N_1(\nu)|} &= - \frac{1}{\left[1 + \frac{N_1(\nu)}{G_0(\nu)H_d(\nu)} \right]^2} \frac{e^{j\theta(\nu)} H_{d+\Delta d}(\nu)}{|G_0(\nu)| H_d^2(\nu)} \\ &\approx - \frac{e^{j\theta(\nu)} H_{d+\Delta d}(\nu)}{|G_0(\nu)| H_d^2(\nu)} \end{aligned} \quad (13)$$

where $\theta(\nu)$ is the phase of the perturbation relative to the signal component $G_0(\nu)$. The approximation in the right hand side of Eq. (13) is for the case that $|N_1(\nu)|$ is small compared to $|G_0(\nu)H_d(\nu)|$.

From $\hat{H}(\nu)$ the parameter \hat{d} is derived, leading (Eq. 1) to the depth estimate \hat{u} . Therefore, the error due to the perturbation propagates to \hat{d} and consequently to \hat{u} . Note that

$$\frac{\partial \hat{u}(\nu)}{\partial |N_1(\nu)|} = \frac{\partial \hat{u}}{\partial f(\hat{u})} \frac{\partial f(\hat{u})}{\partial |N_1(\nu)|}. \quad (14)$$

In the following analysis we use $\partial f(u)/\partial |N_1|$ as a measure for the response to perturbations. We make do with analyzing the influence of the perturbations on the estimation of $f(u)$ since it is simpler and it is easily related to depth by Eq. (1). Since the estimation will be frequency-dependent, we write

$$\frac{\partial f(\hat{u}, \nu)}{\partial |N_1(\nu)|} = \frac{\partial \hat{H}(\nu)}{\partial |N_1(\nu)|} \cdot \left[\frac{\partial \hat{H}(\nu)}{\partial f(\hat{u})} \right]^{-1}. \quad (15)$$

For small perturbations we assume that $\hat{H}(\nu) \approx H(\nu)$, so Eq. (15) becomes

$$\frac{\partial f(\hat{u}, \nu)}{\partial |N_1(\nu)|} \approx C \frac{H_{d+\Delta d}(\nu)}{\frac{\partial H_{d+\Delta d}(\nu)}{\partial d} H_d(\nu) - \frac{\partial H_d(\nu)}{\partial d} H_{d+\Delta d}(\nu)}, \quad (16)$$

where

$$C \equiv - \frac{e^{j\theta(\nu)}}{|G_0(\nu)|}. \quad (17)$$

According to Eqs. (13) and (16), if $H_{d+\Delta d}(\nu) = 0$ for some frequency ν , a perturbation $N_1(\nu)$ does not affect the estimation.

If $|H_d(\nu)| \ll |H_{d+\Delta d}(\nu)|$ we define the transfer function between the images as the reciprocal of Eq. (7):

$$H^{-1}(\nu) = \frac{H_d(\nu)}{H_{d+\Delta d}(\nu)}, \quad \widehat{H}^{-1}(\nu) = \frac{H_{\hat{d}}(\nu)}{H_{\hat{d}+\Delta d}(\nu)}. \quad (18)$$

This takes care of the cases in which $H_d(\nu) = 0$ but $H_{d+\Delta d}(\nu) \neq 0$. Eq. (11) can then be written as

$$\widehat{H}^{-1}(\nu) = H^{-1}(\nu) + \frac{N_1(\nu)}{G_0(\nu)H_{d+\Delta d}(\nu)}. \quad (19)$$

The perturbation causes the estimated transfer function to change:

$$\frac{\partial \widehat{H}^{-1}(\nu)}{\partial |N_1(\nu)|} = \frac{e^{j\theta(\nu)}}{|G_0(\nu)|H_{d+\Delta d}(\nu)}. \quad (20)$$

Calculating the influence on the depth estimation based on this form of the transfer function, we arrive at the same relation as Eq. (16) without assuming the perturbation $|N_1(\nu)|$ to be small relative to $|G_0(\nu)H_d(\nu)|$.

We use the pillbox point spread function (PSF) model [11, 12, 21], since it is valid for aberration-free geometric optics, and has been shown to be a good approximation for large defocus [7, 10, 20]. In this model

$$H_d(\nu) = 2 \frac{D^2}{D_0^2} \frac{J_1(\pi\nu d)}{\pi\nu d}, \quad (21)$$

where D_0 is the diameter of the arbitrarily small aperture being used to mimic the pinhole in the conceptual generation of G_0 . We note that when the sensor is axially moved, the light gathered by the system remains unchanged since D is the same for all the images acquired. Using the relation

$$\frac{\partial [J_1(\xi)/\xi]}{\partial \xi} = - \frac{J_2(\xi)}{\xi} \quad (22)$$

Eq. (16) takes a relatively simple form,

$$\begin{aligned} \frac{\partial f(\hat{u}, \nu)}{\partial |N_1(\nu)|} &\approx -C \frac{D_0^2 d}{D^2} \cdot \\ &\cdot \frac{J_1[\pi\nu(d + \Delta d)]}{J_2[\pi\nu(d + \Delta d)]J_1(\pi\nu d) - J_2(\pi\nu d)J_1[\pi\nu(d + \Delta d)]}. \end{aligned} \quad (23)$$

At high frequencies ν (or at large blur-diameters d), Eq. (23) becomes

$$\begin{aligned} \frac{\partial f(\hat{u}, \nu)}{\partial |N_1(\nu)|} &\approx -C \frac{D_0^2}{D^2} \frac{\pi d \sqrt{\nu d}}{2\sqrt{2}} \cdot \\ &\cdot \frac{\sin[\pi\nu(d + \Delta d) - (\pi/4)]}{\sin(\pi\nu\Delta d)} \end{aligned} \quad (24)$$

where we used the relation

$$J_\mu(\xi) \xrightarrow{\xi \rightarrow \infty} \sqrt{2/(\pi\xi)} \cos[\xi - \mu(\pi/2) - (\pi/4)]. \quad (25)$$

A similar relation is obtained in case a perturbation N_2 is present in G_2 rather than in G_1 :

$$\begin{aligned} \frac{\partial f(\hat{u}, \nu)}{\partial |N_2(\nu)|} &\approx C \frac{D_0^2}{D^2} \frac{\pi(d + \Delta d) \sqrt{\nu(d + \Delta d)}}{2\sqrt{2}} \cdot \\ &\cdot \frac{\sin[\pi\nu d - (\pi/4)]}{\sin(\pi\nu\Delta d)}. \end{aligned} \quad (26)$$

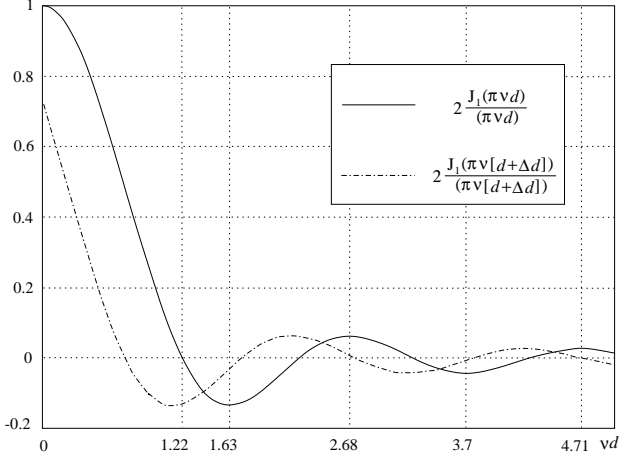


Figure 2. [Solid line] The attenuation of a frequency component ν between a focused and a defocused image as a function of the diameter of the blur kernel d . The horizontal axis is scaled by ν . [Dashed line] The attenuation of the same frequency component when the focus settings are changed so that the blur diameter is $d + \Delta d$, for the case $\Delta d = 1/(2\nu)$.

3. Optimal axial interval

To appreciate the significance of Eqs. (24,26), observe that the reliability of the defocus estimation at high frequencies is optimized (for unknown u hence for unknown d) if

$$|\nu\Delta d| = 0.5, 1.5, 2.5 \dots \quad (27)$$

There, the magnitude of the term $\sin(\pi\nu\Delta d)$ in the denominator is maximal, minimizing the effect of the perturbation on the estimation $\hat{d} = f(\hat{u}, \nu)$. Thus, if DFD is implemented by changing the focus settings, the change (e.g. the axial movement of the sensor) is optimized if it causes the blur-diameter to change according to Eq. (27), where ν is the high frequency component used. Alternatively, if Δd is given, Eq. (27) indicates the optimal frequency components for depth estimation. The optimal Δd was used in Fig. 2, that shows the normalized $H_d(\nu)$ (21) of the pill-box model, at a specific frequency ν , as a function of the blur-diameter d . Fig. 2 also shows $H_{d+\Delta d}(\nu)$. Note that at high frequencies or defocus, the Bessel function resembles a cosine function (25), and the two functions are out of phase by $\pi/2$. Hence, in this situation extrema of H_d are at zero-crossings of $H_{d+\Delta d}$ and vice-versa. Thus, these values of $\nu\Delta d$ maximize the ratio between these functions (or its reciprocal).

On the other hand, if

$$|\nu\Delta d| = 1, 2, 3 \dots \quad (28)$$

the denominator of Eqs. (24,26) is zero. In this situation the estimation is highly ill-conditioned. Note that as the axial interval is increased, hence Δd is increased, for a given scene, the number of useful frequency components that satisfy Eq. (27) and the number of problematic components that satisfy Eq. (28) both increase.

Suppose that the highest frequency in the image is ν_{max} . Then Eq. (28) dictates that for stable estimation of all frequency components, Δd must satisfy

$$\Delta d < \frac{1}{\nu} \leq \frac{1}{\nu_{max}} = 2\Delta x, \quad (29)$$

where Δx is the inter-pixel period of the sensor and we assumed that $\nu_{max} = 1/(2\Delta x)$ (the Nyquist rate). However, according to Eq. (27), in order to obtain reliable results, one should use an axial interval leading to a change in the blur-diameter that is at least half that written in Eq. (29), that is, one inter-pixel spacing. Thus *the change of the focus settings that leads to robust and accurate estimation corresponds to a change in the blur diameter that is bounded by*

$$\Delta x \leq \Delta d < 2\Delta x. \quad (30)$$

Eq. (30) can be interpreted to reveal a new property of depth of field (DOF). The depth of field of the system is the range of distances u around the focused distance \tilde{u} in which the defocus blur is undetectable. This depends on the inter-pixel distance Δx [1, 3] and on the blur-diameter d : the blur can be sensed when $d \sim \Delta x$ or larger. d depends on $\tilde{u} - u$ and the system dimensions. When using the threshold value $\Delta d = \Delta x$, if one of the images is in focus (having $d = 0$), the blur kernel in the other image will have a diameter $d_{th} = 0 + \Delta d = \Delta x$. Thus, using $\Delta d < \Delta x$ is an attempt to sense defocus (generally, change of defocus) for changes in distance that are smaller than the DOF. Hence, *sampling the axial position in DOF intervals (for which $\Delta d = \Delta x$) is optimal with respect to robustness to perturbations at the Nyquist frequency*. Changing the focus setting by a smaller axial interval means that no frequency in the image will satisfy the optimality condition (27). Changing the focus setting by a larger axial interval will be sub-optimal for the Nyquist frequency, but will be optimal for some lower frequency. If the interval of the axial position is twice than the DOF or more, there will be some frequency components in the image, for which estimation will be unstable (28). We note that sampling depth at DOF intervals is known to be efficient [9], particularly in depth from *focus* algorithms [1, 18]. Here we showed that DOF sampling is also a meaningful threshold for robust operation of DFD algorithms.

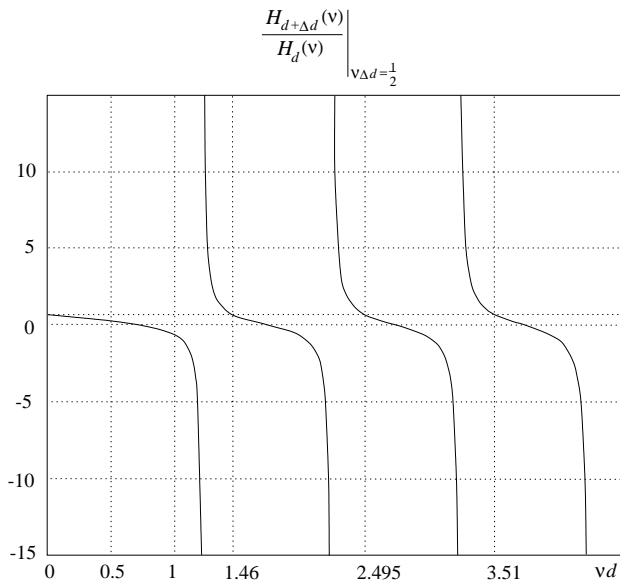


Figure 3. Two images are acquired with different focus settings. The transfer function between the images is the ratio between their individual frequency responses (relative to the focused state), plotted in Fig. 2. In the DOF threshold $\Delta d = 1/(2\nu)$, the width of the band without ambiguities satisfies $\nu d \approx 1.46$. For infinitesimal Δd this width satisfies $\nu d \approx 1.63$.

4. Uniqueness and stability

DFD infers depth by the comparison of images taken with different defocus blurring. If the defocus change is achieved by change of the focus settings, then basically, DFD estimates d from measurement of the ratio H (Eq. (7)). From \hat{d} , the depth u is derived. Implicitly, DFD algorithms fuse information from several frequency bands.

To have a unique solution, we should check the uniqueness of the estimation of d . Fig. 3 plots H for the case $\Delta d = 1/(2\nu)$, that is, the ratio of the two functions plotted in Fig. 2. Each ratio between these responses can be yielded by many diameters d , as it is not one-to-one. The lowest band for which the ratio is one-to-one in this figure is $0 < \nu d < 1.46$. However, if the axial increments of the sensor position are smaller, this bandwidth broadens. As Δd is decreased, the responses shown in Fig. 2 converge. Convergence is fastest near the local extrema of $H_d(\nu)$. Hence, as $\Delta d \rightarrow 0$ the lowest band in which the matching (correspondence) ambiguity is avoided is between the two first local extrema, i.e.,

$$0 < \nu d < 1.63 . \quad (31)$$

However, according to Eqs. (24,26), if $\Delta d \rightarrow 0$ the estimation becomes unstable. If we use the guideline (27) Fig. 3

(where $\nu \Delta d = 0.5$) shows that for unambiguous *and* stable estimation

$$0 < \nu d < 1.46 . \quad (32)$$

If a coarse estimate of the depth is available (e.g., by using only the band of Eq. (32)), higher frequencies may be used without ambiguity problems, as suggested in [16]. Then, unstable frequency components exist (Eq. 28) and filtering them out improves the estimation.

Simulation and experimental results reported in [21] support the results of our analysis. In the DFD method suggested in [21], the defocus change between acquired images was obtained by changing the focus settings. The images were then filtered by several band pass operators, and the ratios of their outputs were used to fit a model. The ratios are actually a function of the transfer function defined in Eq. (7) between the images. The authors of [21] noticed that the solution may be ambiguous due to the nonmonotonicity of the ratios, as a function of the frequency and the blur diameter. They thus limited the band used to the first zero crossing of the pillbox model (21) which occurs at $\nu d = 1.22$ ($\nu r = 0.61$). However, their tests revealed that the frequency band can be extended by about 30%, i.e., to $\nu d \approx 1.6$. This is in agreement with the bound for unique solution set by Eq. (31), i.e. $\nu d = 1.63$.

For reasons of numerical stability (measured by the behavior of the Newton-Raphson algorithm for estimation), the frequency band limit was actually set in [21] to $\nu d = 1.46$ (i.e., $\nu r = 0.73$). Within this band the results came out to be stable, while beyond it the range estimation became unstable. Note that this is in excellent agreement with Eq. (32).

5. Discussion

We analyzed the effect of perturbations on DFD estimation, by examining their influence in each spatial frequency component of the images. Estimation that relies on certain frequency components is most robust, while the contribution of other frequencies is very sensitive to perturbations. A possible application of this theoretical framework would be an algorithm that relies on a coarse estimate of the blur diameter to select the optimal spatial frequencies (for which the response to perturbations is minimal) to obtain a fine estimate.

In DFD estimation based on a spectral component with frequency ν , the axial movement of the sensor is optimal if it causes the change Δd in the blur diameter to satisfy $|\nu \Delta d| = 0.5, 1.5, 2.5 \dots$. Using the DOF as the axial interval is optimal with respect to robustness to perturbations at the Nyquist frequency. Using an axial interval which is twice or more than that, can lead to unstable results at some frequency components.

In telecentric systems, Δd is independent of the depth and invariant on axial shifts of the plane of best focus. Thus Δd has a linear and constant relation to the axial interval of the sensor position: $\Delta v = F \Delta d / D$. Therefore the results obtained in this work can be easily applied to such systems. Generally, if the system is not telecentric, Δd (and thus the preferable frequencies) depends on the depth we wish to estimate, and which may not be spatially constant. In these cases, axial shift invariance of Δd may be initially assumed, and a coarse depth estimate will indicate the deviation from this assumption. Consequent estimation of the true Δd may serve as a guideline for improving the depth estimate using the corresponding optimal frequencies.

The presence of unstable frequency components, in which the denominator of Eq. (16) is zero, is related to local extrema of the defocus transfer function. Unmonotonic transfer functions are theoretically predicted in [5, 10, 20] and measured in [8]. Thus our analysis provides guidelines for determining the optimal intervals and frequencies in a broad range of defocus PSF's.

The analysis in this paper is essentially deterministic. However, the presence of independent noise in both of the acquired images simultaneously, at all spatial frequencies, may be better analyzed in a stochastic framework that is based on the deterministic analysis presented here. In [15] stochastic methods have been used. Comparison and integration of the two approaches is an interesting topic for future research.

This research was carried out in the Ollendorff Center of the Department of Electrical Engineering, Technion, and in the Department of Electrical Engineering - Systems, Faculty of Engineering, Tel-Aviv University. It was funded in part by the Israeli Ministry of Science.

References

- [1] A. L. Abbott and N. Ahuja, "Active stereo: integrating disparity, vergence, focus, aperture and calibration for surface estimation," *IEEE Trans. PAMI* **15** pp. 1007-1029 [1993].
- [2] V. M. Bove Jr., "Discrete fourier transform based depth-from-focus," *Image Understanding and Machine Vision 1989. Technical Digest Series* **14**, Conference ed., pp. 118-121 [1989].
- [3] K. Engelhardt and G. Hausler, "Acquisition of 3-D data by focus sensing," *App. Opt.* **27**, pp. 4684-4689 [1988].
- [4] J. Ens and P. Lawrence, "An investigation of methods for determining depth from focus," *IEEE Trans. PAMI* **15**, pp. 97-108 [1993].
- [5] A. R. FitzGerrell, E. R. Dowski, Jr. and T. Cathey, "Defocus transfer function for circularly symmetric pupils" *App. Opt.* **36**, pp. 5796-5804 [1997].
- [6] S. Hiura, G. Takemura and T. Matsuyama, "Depth measurement by multi-focus camera," *Proc. of Model-Based 3D Image Analysis*, pp. 35-44 [Mumbai 1998].
- [7] H. H. Hopkins, "The frequency response of a defocused optical system," *Proc. R. Soc. London Ser. A* **231** pp. 91-103 [1955].
- [8] W. N. Klarquist, W. S. Geisler and A. C. Bovic, "Maximum-likelihood depth-from-defocus for active vision," *Proc. Inter. Conf. Intell. Robots and Systems: Human Robot Interaction and Cooperative Robots*, vol. 3, pp. 374-379 [Pittsburgh 1995].
- [9] A. Krishnan and N. Ahuja, "Panoramic image acquisition," *Proc. CVPR*, pp. 379-384 [San-Francisco 1996].
- [10] H. C. Lee, "Review of image-blur models in a photographic system using the principles of optics," *Opt. Eng.* **29**, pp. 405-421 [1990].
- [11] S. K. Nayar, M. Watanabe and M. Nogouchi, "Real time focus range sensor," *Proc. ICCV*, pp. 995-1001 [Cambridge 1995].
- [12] M. Noguchi and S. K. Nayar, "Microscopic shape from focus using active illumination," *Proc. ICPR-A*, pp. 147-152 [Jerusalem 1994].
- [13] A. P. Pentland, "A new sense for depth of field," *IEEE Trans. PAMI* **9**, pp. 523-531 [1987].
- [14] A. Pentland, S. Scherock, T. Darrell and B. Girod, "Simple range camera based on focal error," *J. Opt. Soc. Amer. A* **11**, pp. 2925-2934 [1994].
- [15] A. N. Rajagopalan and S. Chaudhuri, "Optimal selection of camera parameters for recovery of depth from defocused images," *Proc. CVPR*, pp. 219-224 [San Juan 1997].
- [16] Y. Y. Schechner and N. Kiryati, "Depth from Defocus vs. Stereo: How Different Really are They?" *Proc. ICPR*, pp. 1784-1786 [Brisbane 1998].
- [17] Y. Y. Schechner and N. Kiryati, "Depth from Defocus vs. Stereo: How Different Really are They?" *EE-PUB-1155*, Technion - Israel Institute of Technology. Accepted to the *IJCV*.
- [18] Y. Y. Schechner, N. Kiryati and R. Basri, "Separation of transparent layers using focus," *Proc. ICCV*, pp. 1061-1066 [Mumbai 1998].
- [19] S. Scherock, "Depth from defocus of structured light," *TR-167*, Media-Lab, MIT [1991].
- [20] G. Schneider, B. Heit, J. Honig and J. Bremont, "Monocular depth perception by evaluation of the blur in defocused images," *Proc. ICIP*, vol. 2, pp. 116-119 [Austin 1994].
- [21] M. Watanabe and S. K. Nayar, "Minimal operator set for passive depth from defocus," *Proc. CVPR* pp. 431-438 [San Francisco 1996].